A KINETIC STUDY ON THE CARBOTHERMIC REDUCTION OF ZINC OXIDE FROM ELECTRIC ARC FURNACE DUST

M. Sheikhshab Bafghi*, M. Karimi and M. Adeli

* *msbafghi@iust.ac.ir*

Received: April 2013 **Accepted: October 2013**

School of Metallurgical & Materials Engineering, Iran University of Science and Technology (IUST), Narmak, Tehran, Iran

Abstract:*In the present study, reduction of zinc oxide from the pellets made of steelmaking electric arc furnace dust has been investigated. Effects of such parameters as the type of carbon material (graphite, coke and charcoal) as well as time and temperature on the reduction reaction have been examined. The reduced (dimensionless) time method was applied to perform a kinetic analysis of the system. Experimental results showed that increasing the temperature in the range of 925-1150°C results in a remarkable increase in the reduction rate. It was also shown that the reduction process is controlled by chemical reaction. Meaningful difference in the activation energy values calculated for reduction with graphite (24.75 kcal/mol), coke (18.13 kcal/mol) and charcoal (11.52 kcal/mol) indicate the predominant role of chemical reaction (carbon gasification) in the overall reaction rate and its rate-controlling mechanism. Carbothermal reduction of pelletized EAF dust proved to be an efficient reduction method, so that above 90% reduction was achieved in about one hour at temperatures around 1100°C.*

Keywords: *Electric arc furnace dust, zinc oxide carbothermic reduction, pelletizing, kinetics, mechanism, activation energy*

1. INTRODUCTION

Electric arc furnaces (EAF) are extensively used in the steelmaking industry. EAF steelmaking dust contains considerable amounts of zinc, making it a valuable secondary source of this metal. Around 20 kg of dust is collected per tonne of steel produced in electric arc furnaces [1]. The filtered dust is categorized as a hazardous waste in most countries as it contains heavy metals. On the other hand, recovery of valuable metals through adequate processing is of importance from both economic and environmental viewpoints.

The characterization, minimization, and precise utilization of EAF dust including recovery of the worthy constituents, have been the subject of many studies [1-9]. Several techniques have been proposed for the recovery of zinc from EAF dust based on hydrometallurgical processes [10-16], selective reduction by solid iron [17, 18], selective chlorination [19], thermal treatment with PVC [20], lime addition and magnetic separation process [21] and carbothermic reduction [22-25]. Among the most recent studies on the carbothermic reduction of zinc oxide in EAF dust, Kim et al. [24] have studied the effect of various additives such as Fe_2O_3, $CaCO_3$, and mill scale on the kinetics of this reaction. In their study, mixtures of loose powders of starting materials contained in a covered alumina crucible were used. They deduced that all three additives enhance the reaction rate of zinc oxide with carbon, $CaCO_3$ being the most effective one. They used the shrinkage core model to calculate and compare the reaction activation energies in the absence and presence of additives. Chen [23] used compact samples of ZnO/carbon mixture to study the reduction reaction under a nitrogen atmosphere and reported that the reduction rate increases by increasing the C/ZnO molar ratio, height and density of solid sample and reaction temperature, as well as by decreasing the ZnO and carbon particle size.

The main objective of the present research work has been the kinetic study of zinc oxide carbothermal reduction in EAF dust in order to clarify the reaction rate and mechanism. For this purpose different carbon materials, including charcoal, coke and graphite have been examined. A unique feature of the present study is the use of pellets prepared from EAF dust, which were embedded in a bed of different carbon materials.

Furthermore, as another new approach, reduced-time model was used to elucidate the reaction kinetics in EAF dust-carbon system.

Experiments were performed at temperatures higher than the boiling point of zinc (907 °C) leading to the evaporation of zinc. Reduction efficiency was estimated through the measurement of the zinc remained in the dust after the elapse of any given time.

2. EXPERIMENTAL PROCEDURE

The EAF dust used in the present study was obtained from Yazd Alloy Steelmaking Company (Yazd, Iran). Wet chemical analysis showed that the dust contained 12.49 wt% Zn.

A Bruker D8 Advance X-ray diffractometer with Cu kα radiation (λ = 1.54178 A˚) at a scan rate of 0.02°/s was used to determine the mineralogical characterization of as-received dust, as well as its post-reduction specification. XRD pattern of the raw EAF dust sample is shown in Fig. 1. The main zinc-containing phases present in the sample were distinguished as $ZnO.Fe_2O_3$ (franklinite) and ZnO.

As mentioned earlier, a unique feature of the present study has been the use of pellets made from fine powders of raw materials. Pellets of 12 mm diam. were manually made from the dust by adding bentonite (~%2) and water (10-15%). As-made pellets were dried in a laboratory oven dryer through a three stage drying process at temperatures of 100, 150, and 200 ˚C, each step for about one hour. A stainless steel crucible was used as the container of a carbon bed in which the pellets were embedded. Coarser coal particles were used to cover the carbon bed on the top. The reduction process was performed by heating the samples in a muffle furnace at appropriate temperatures for certain time durations. Graphite, coke, and charcoal were used as reducing agents. The reduction process was performed at different temperatures of 925, 1000, 1075, and 1150 ˚C. Five experimental tests for 10, 20, 30, 45, and 60 minutes were performed at each specific temperature. Zinc content of the reduced samples was measured using atomic-absorption spectrophotometry (AAS) method and the reduction efficiency was calculated using the following relationship:

$$R\,(\%) = \left(\frac{W_0 - W_t}{W_0}\right)\times 100 = \left(\frac{P_0 m_0 - P_t m_t}{P_0 m_0}\right)\times 100 \qquad (1)$$

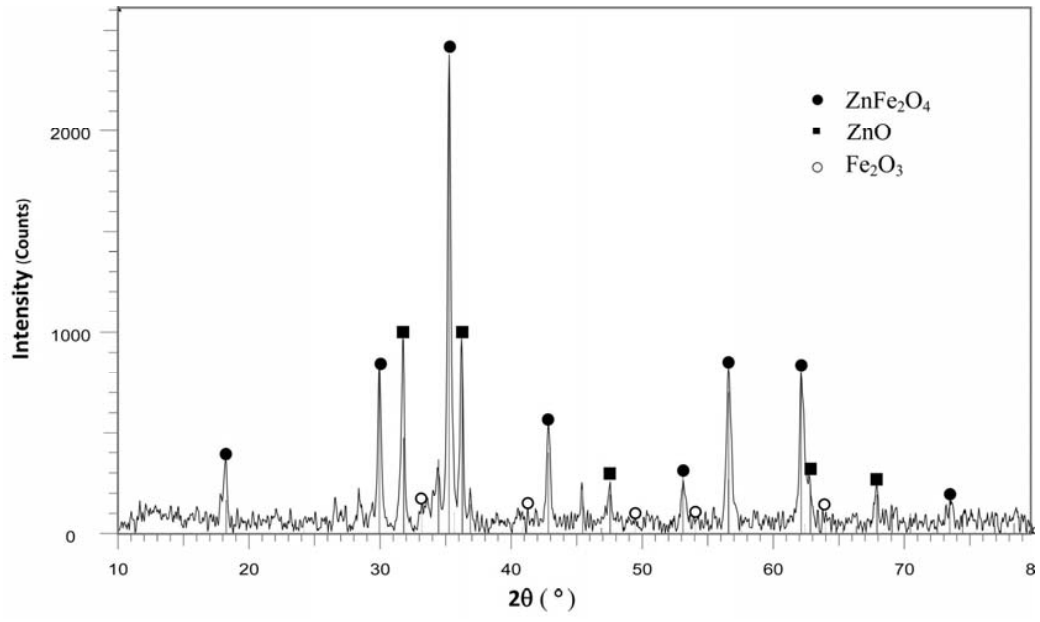

Fig. 1. XRD pattern of the steelmaking electric arc furnace dust.

where W_o is the initial zinc content of the pellet, W_t the zinc content in the reduced pellet, m_o the initial mass of the pellet, m_t the post-reduction mass, P_o the mass percent of zinc in the initial pellet and P_t the zinc mass percent in the reduced sample.

3. RESULTS AND DISCUSSION

The overall reaction of the carbothermic reduction of zinc oxide is in the following form:

$$2ZnO(s) + C(s) = 2Zn\ (g) + CO_2(g) \quad (2)$$

However, it is believed this solid-solid reaction proceeds by CO gas produced through carbon gasification or Boudouard reaction. Therefore, the probable gas-solid reactions occurring during the reduction of EAF dust can be written in the following forms:

$$ZnFe_2O_4(s) + 3CO\ (g) = ZnO(s) + 2Fe(s) + 3CO_2(g) \quad (3)$$

$$ZnO(s) + CO\ (g) = Zn(g) + CO2(g) \quad (4)$$

$$C(s) + CO_2(g) = 2CO(g) \quad (5)$$

With regard to the above reactions, the reduced sample contains a large amount of metallic iron, as will be shown in the relative XRD pattern in the following sections. As above reactions reveal, main influencing parameters are temperature and type of reductant (carbon material). Experimental results showed no appreciable effect with regard to the particle size of carbon materials.

3. 1. The Effect of Reductant Type

As mentioned before, effect of the type of carbon material on the reduction efficiency was evaluated using three different carbon materials, i.e., graphite, coke and charcoal. The reduction efficiency vs. time at various temperatures is presented in Figs. 2-5 for different reducing agents.

As shown in these figures, type of the carbon material has a significant effect on the reduction efficiency at all experimental temperatures. The lowest reduction efficiency is obtained by graphite while charcoal yields the highest efficiency; the efficiency obtained by coke stands in-between. Hence, it could be deduced that the reduction rate depends on the rate of CO

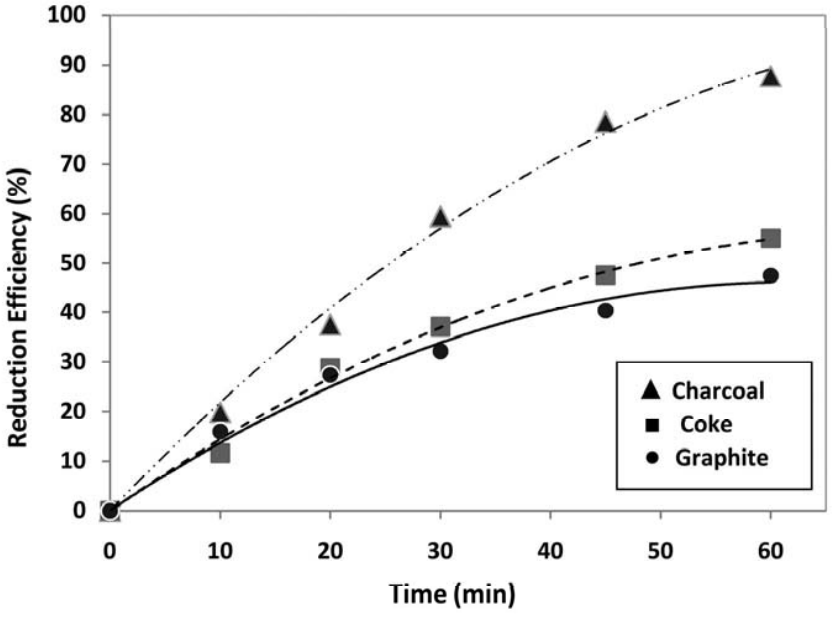

Fig. 2. Effect of the type of carbon material on the reduction efficiency at 925°C.

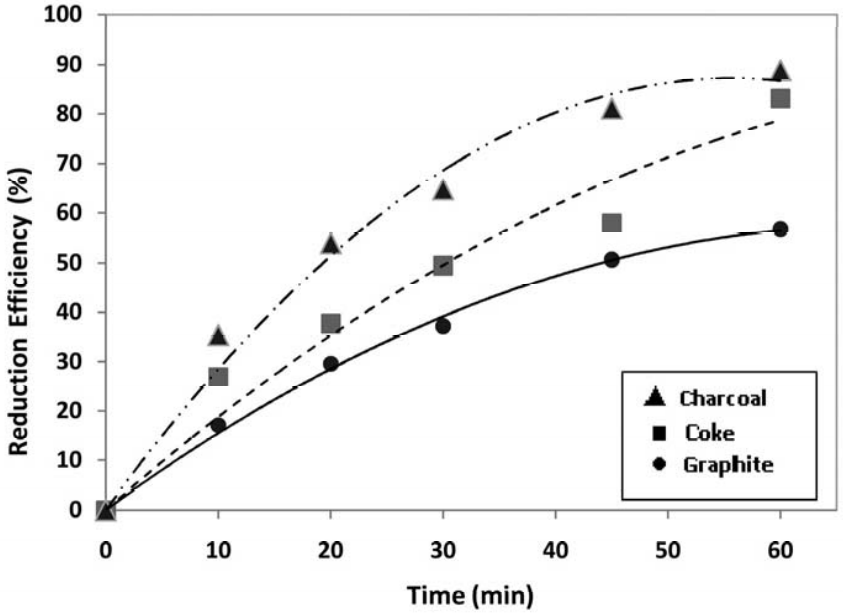

Fig. 3. Effect of the type of carbon material on the reduction efficiency at 1000 °C.

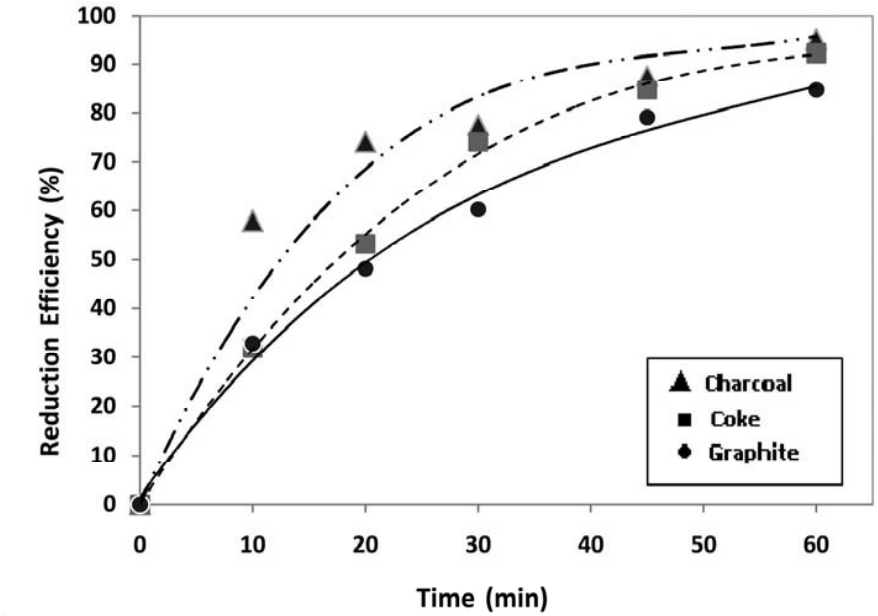

Fig. 4. Effect of the type of carbon material on the reduction efficiency at 1075 °C.

generated from the reaction of CO_2 and C according to Boudouard reaction, whose rate increases with increasing the reactivity of carbon material.

3. 2. The Effect of Temperature

Figs. 6-8 show the effect of temperature on the reduction efficiency for three types of carbon material.

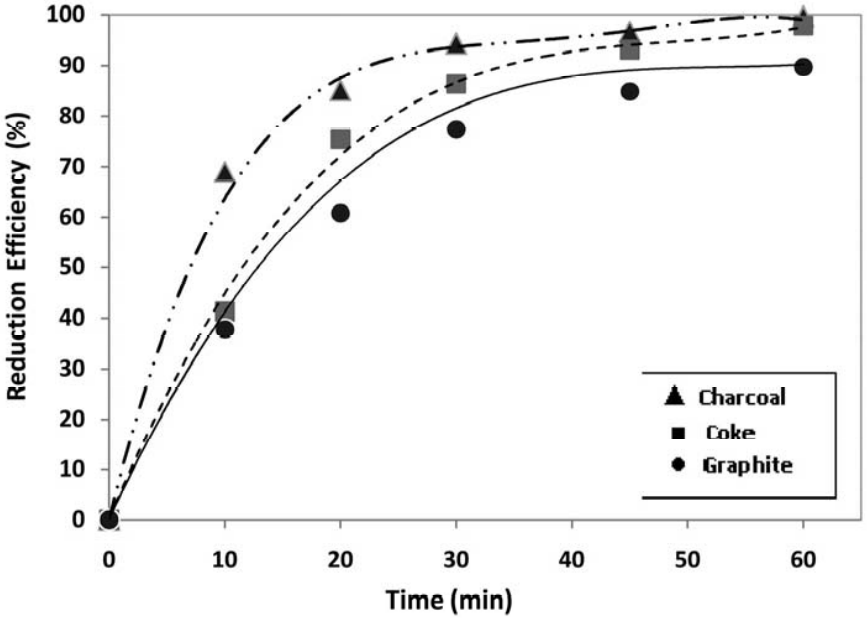

Fig. 5. Effect of the type of carbon material on the reduction efficiency at 1150 °C.

Again, it can be observed that an increase in the temperature remarkably accelerates the reduction process, regardless the type of carbon material. Considering the high sensitivity of the reaction rate to the experimental temperature, it may be concluded that the chemical reaction has a predominant role in the reaction kinetics. Higher temperature dependency of the reaction rate at lower temperatures, as the figures show, also supports a chemical rate controlling mechanism.

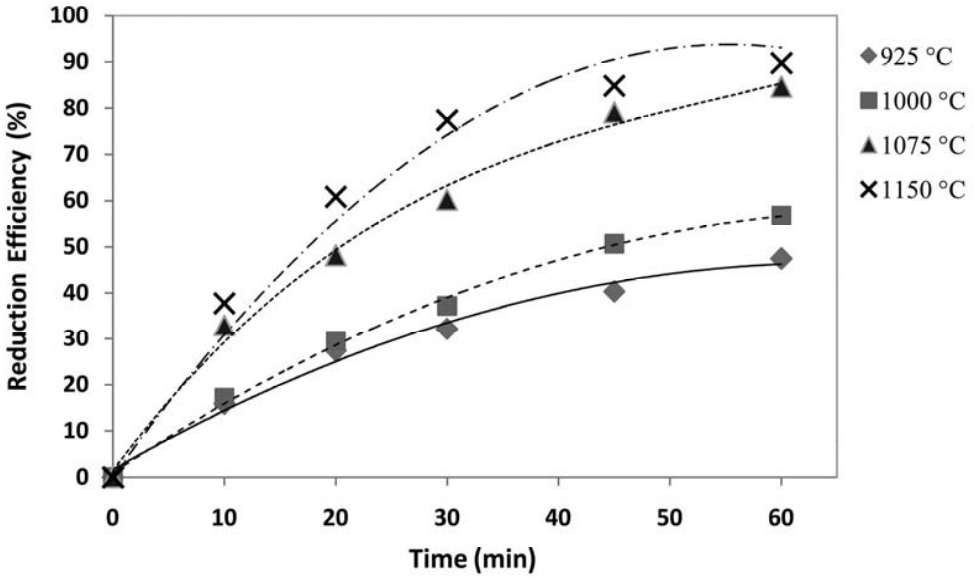

Fig. 6. Effect of temperature on the reduction efficiency using graphite as the carbon material.

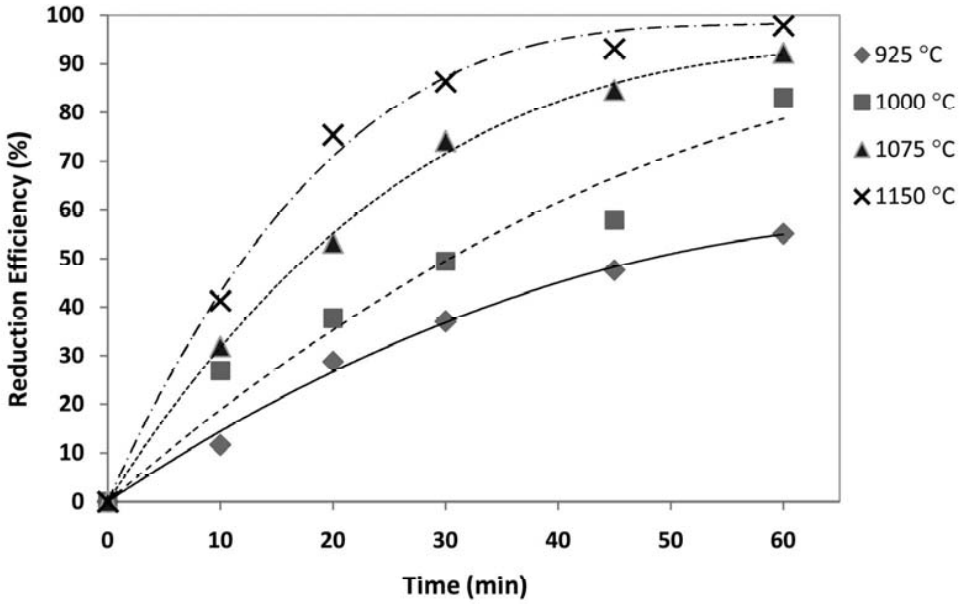

Fig. 7. Effect of temperature on the reduction efficiency using coke as the carbon material.

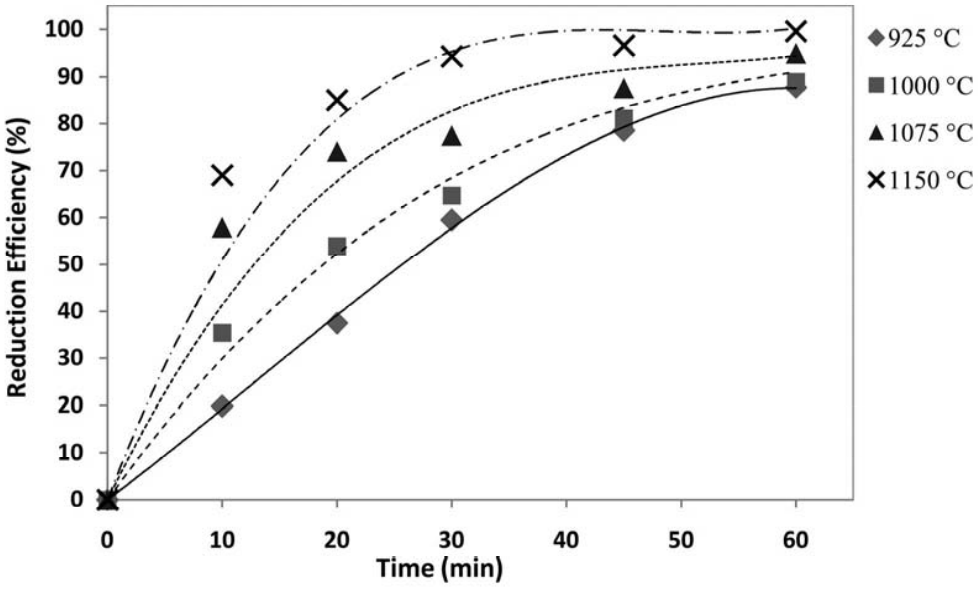

Fig. 8. Effect of temperature on the reduction efficiency using charcoal as the carbon material.

3. 3. Characterization of a Typical Reduced Sample

XRD analysis of the reduced samples showed that there are no detectable zinc-bearing phases remaining in the samples reduced under optimum conditions (using the most available reductant (coke), temperature: about 1100 °C, time: 1h) with a reduction efficiency around 95%. A typical XRD pattern of a reduced sample is presented in Fig. 9, which shows that Fe and Ca_2SiO_4 are the

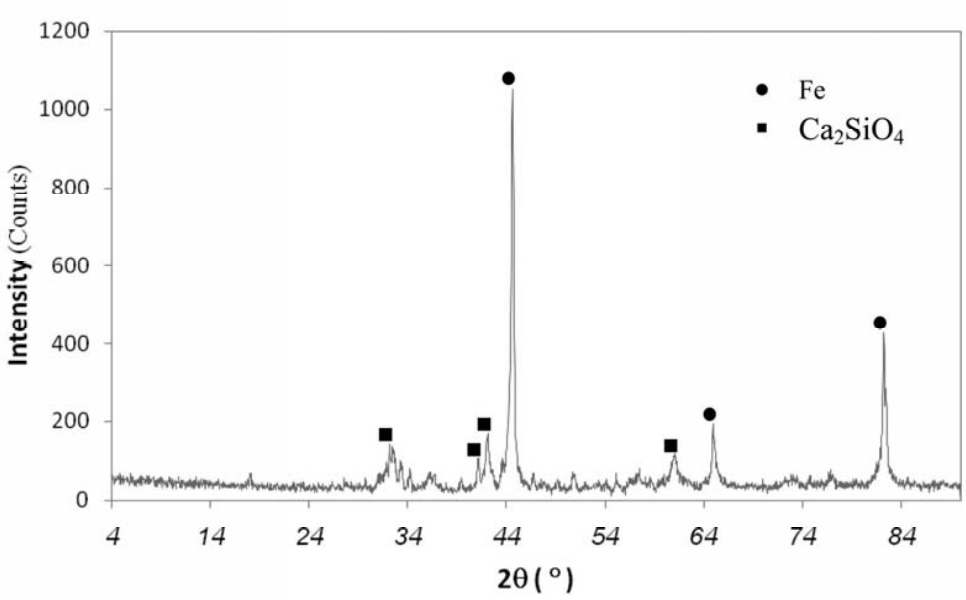

Fig. 9. XRD pattern of a typical 95% reduced sample.

main existing phases in the reduced product. Wet chemical analysis showed the amount of zinc in this reduced sample to be less than 0.02wt%.

3. 4. Kinetic Analysis

The main steps through which the steelmaking EAF dust is reduced by carbon may be considered as follows:

1. Diffusion of CO gas molecules through the gas boundary layer towards the dust particles
2. Inward diffusion of CO through the product layer (ash layer) around the dust particles
3. Carbothermal reduction of zinc oxide at the surface of unreacted core according to reaction 4
4. Outward diffusion of CO_2 molecules through the product layer
5. Diffusion of CO_2 through the gas phase boundary layer to the surface of carbon particles
6. Gasification of carbon by CO_2 and regeneration of CO through the Boudouard reaction (reaction 5)

The sequential process depicted above, is repeated again and again. As mentioned earlier, the Boudouard reaction seems to be the most influential step in controlling the rate of the reduction process. If so, it can be assumed that the reduction reaction of zinc oxide in the dust by CO might have a small effect on the overall process rate. Hence, the concentrations of CO and CO_2 at the interface of unreacted core particles have almost constant values close to their equilibrium ones. Since the reaction between C and CO_2 and formation of CO on the carbon particles is the main rate controlling step, the concentrations of CO and CO_2 at the the surface of carbon particles are far from their thermodynamic values. In other words, the amount of CO_2 is higher and the concentration of CO existing at the carbon surface is lower than the equilibrium value.

Reduced (dimensionless) time method proposed by Ray [26] was used in the present study to determine the rate-controlling mechanism of the reaction. In this method, the experimental data are expressed in the general form of $g(\alpha)=kt$, with α being the fraction reacted and t representing the time. The relationship can be rewritten in the following form:

$$g(\alpha) = A\left(\frac{t}{t_{0.5}}\right) \quad (6)$$

where A is a constant depending on the form of

g(α) equation, and $t_{0.5}$ indicates the time of 50 percent conversion. Therefore, a single plot of α-$t/t_{0.5}$ can be used to present the whole data regardless the nature of the system and experimental conditions.

Since mass transfer in the gas phase is sufficiently high at elevated temperatures, the diffusion of gas molecules through the gas boundary layer is not believed to be of a noticeable importance with regard to the controlling mechanism. Heat transfer is also not important due to the small size of the particles. Therefore, either the diffusion of gas through the product layer or chemical reaction (or a combination of both) could be rate-controlling.

g(α) takes the form of equations (7) and (8) for chemical reaction and three-dimensional mass transfer controlling situations, respectively [26]:

$$\text{chemical control: } g_1(\alpha) = 1-(1-\alpha)^{\frac{1}{3}} = k_c'.t \quad (7)$$

$$\text{diffusion control: } g_2(\alpha) = 1-\frac{2}{3}\alpha-(1-\alpha)^{\frac{2}{3}} = k_{d_2}'.t \quad (8)$$

Above kinetic models are changed into the following dimensionless-time equations using the dimensionless-time method:

$$\text{Chemical control: } 1-(1-\alpha)^{\frac{1}{3}} = 0.2063\frac{t}{t_{0.5}} \quad (9)$$

$$\text{Diffusion control: } 1-\frac{2}{3}\alpha-(1-\alpha)^{\frac{2}{3}} = 0.0367\frac{t}{t_0} \quad (10)$$

Comparison of the experimental data (solid black symbols) and values calculated (solid line) by using equations (9) and (10) for chemical-control and three-dimensional diffusion control models is shown in Figs. 10 and 11, respectively.

Comparison of these two plots reveals that experimental data of the present study show a better fitness to the chemical-control model (Fig. 10). In other words, it can be deduced that the chemical-control model explains the experimental data more reasonably and the overall reaction is predominantly governed by the chemical reaction. Similar result was obtained in the carbothermic reduction of celestite [27]. A more clear deduction is possible with reference to the activation energy values.

The slopes of plots of g(α) function vs. time can be used to determine the apparent rate constant for different experimental temperatures and then calculate the activation energy using the

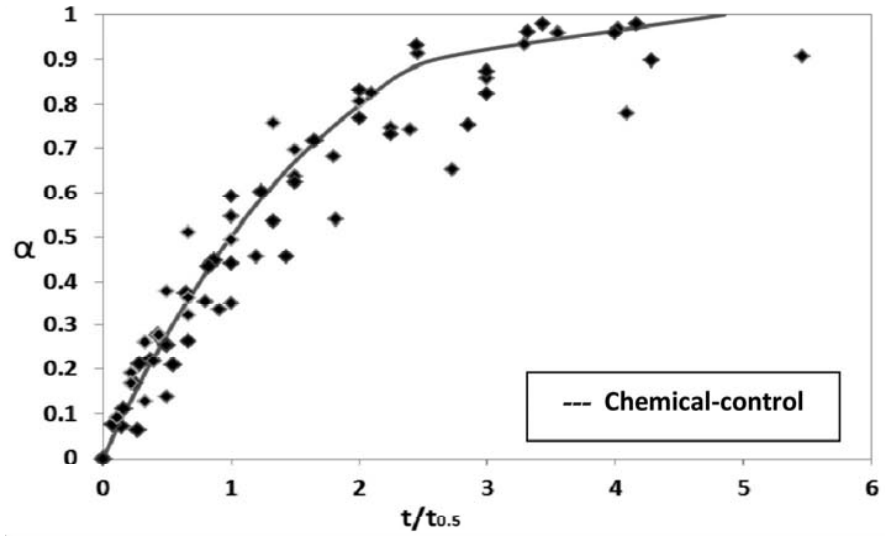

Fig. 10. Plot of α vs. $t/t_{0.5}$ for chemical reaction rate-controlling situation.

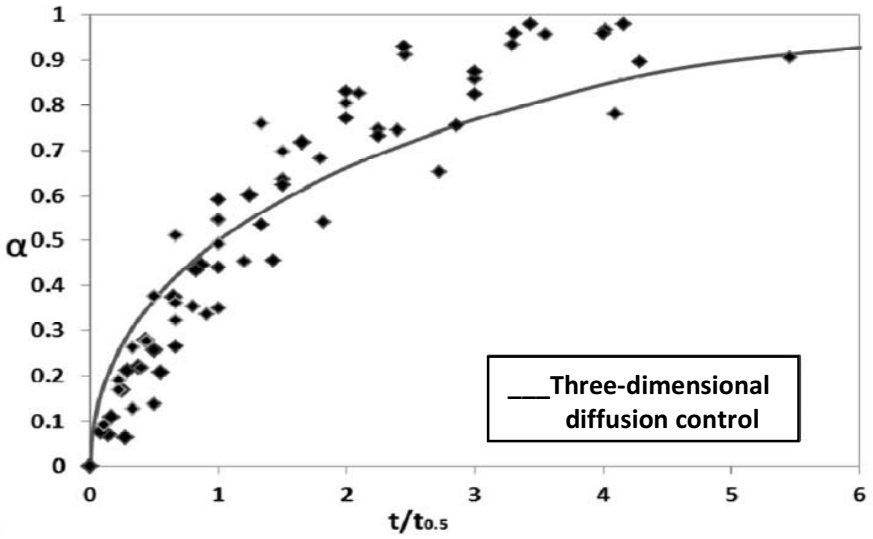

Fig. 11. Plot of α vs. $t/t_{0.5}$ for diffusion rate-controlling situation.

Table 1. Values of rate constant calculated for different reductants.

Temperature (°C)	$k \times 10^3$ (min^{-1})		
	Graphite	Coke	Charcoal
925	1.71	3.02	5.64
1000	3.36	4.90	6.38
1075	5.44	7.05	8.22
1150	6.37	9.28	12.31

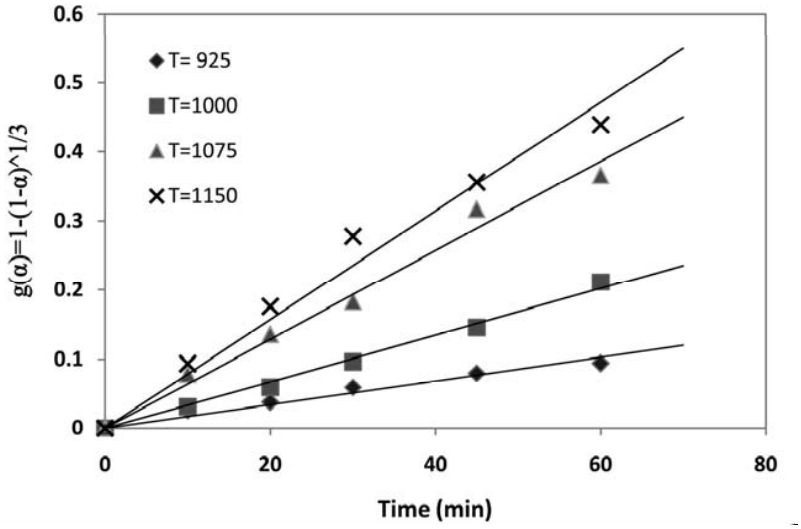

Fig. 12. g(α) function vs. time for chemical-reaction model with graphite as the reducing agent.

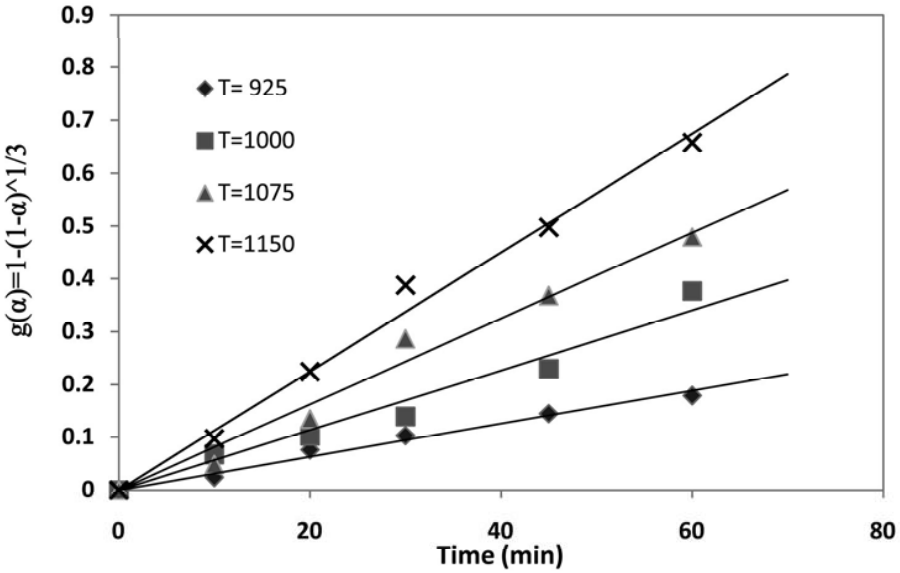

Fig. 13. g(α) function vs. time for chemical-reaction model with coke as the reducing agent.

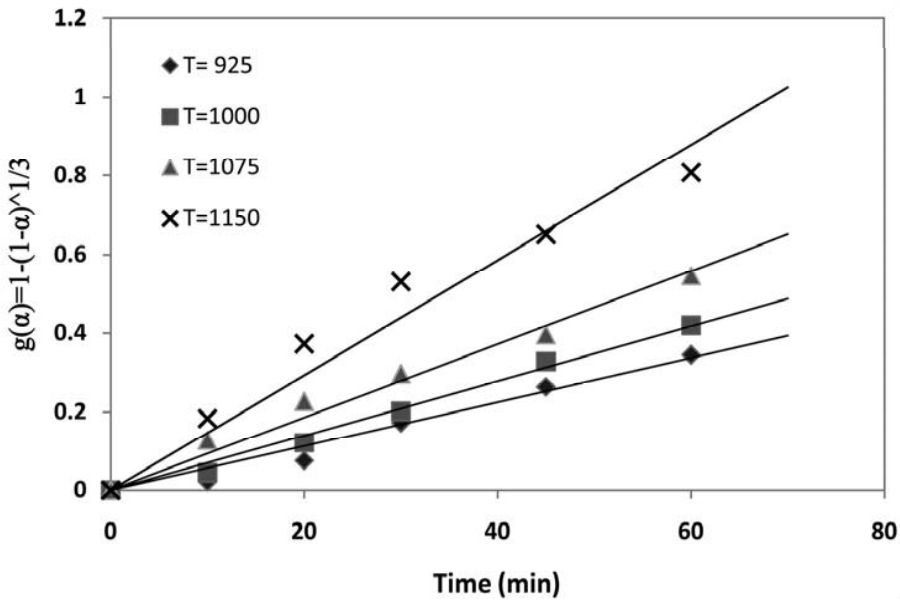

Fig. 14. g(α) function vs. time for chemical-reaction model with charcoal as the reducing agent.

Arrhenius relationship for each reductant. Figs. 12-14 show the g(α) for chemical-control model vs. time for three different types of carbon material and different temperatures. Values of rate constant obtained using these plots are tabulated in Table 1.

Plots of lnk vs. reciprocal absolute temperature for different reductants are presented in Fig. 15. Values of the activation energy calculated from the line slopes in Fig. 15 for graphite, coke and charcoal were 24.75, 18.13 and 11.52 kcal/mol, respectively.

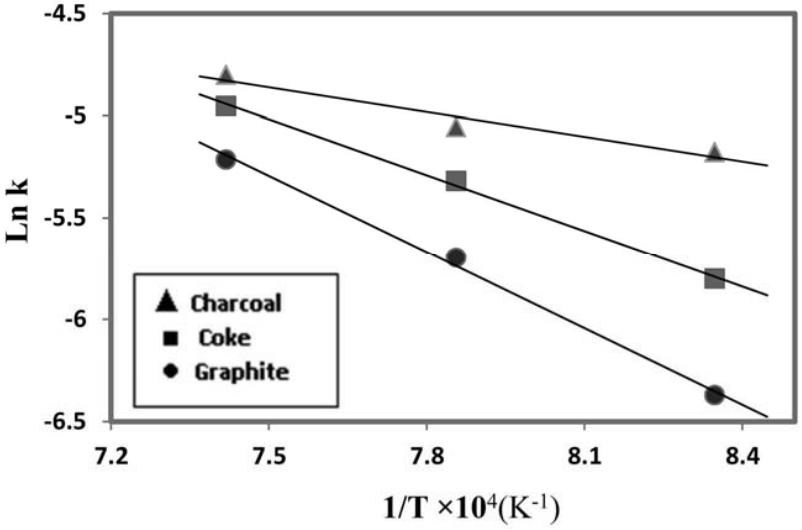

Fig. 15. lnk vs. 1/T for chemical control situation.

A carbon material with the lowest reactivity (graphite) needs the highest activation energy and vice versa. It can be seen that the reactions with graphite and charcoal have the highest and lowest values of activation energy, respectively, and the value of activation energy corresponding to coke stands in between. This is in accordance to the reactivity of these reductants. This provides further evidence for the dependence of reduction rate of zinc oxide in steelmaking EAF dust on the reactivity of carbon material and consequently on the rate of carbon gasification (Boudouard) reaction. The activation energies obtained in the present study are comparable to the values reported by other researchers for the gasification of different types of carbon [28-30], which is another proof of the correctness of the deduced rate-controlling mechanism.

4. CONCLUSIONS

1. Carbothermic reduction of pelletized EAF dust in a carbon bed proved to be an efficient method, so that above 90% reduction can be achieved in about one hour at temperatures around 1100°C.
2. Temperature is recognized as the most effective parameter in the carbothermic reduction of zinc oxide in steelmaking electric arc furnace (EAF) dust. The remarkable effect of temperature on the reduction rate shows the importance of chemical reaction as a rate-controlling step.
3. Analysis of the reaction kinetics using dimensionless-time method showed that the reduction process is mostly chemically-controlled.
4. An increase in the reactivity of carbon material increases the reduction efficiency. This can prove the importance of carbon gasification (Boudouard) reaction in controlling the overall reduction rate. Considerable difference in the values of activation energy calculated in the case of reduction with graphite (24.75 kcal/mol), coke (18.13 kcal/mol), and charcoal (11.52 kcal/mol) reveals the important role of the reductant reactivity and provides further support for the assumed mechanism. Therefore, it can be deduced that the reduction process of zinc oxide in EAF dust is mainly controlled by carbon gasification reaction.

REFERENCES

1. Sofilic, T., Mioc, A. R.,Stefanovic, S. C., Radovic, V. N., and Jenko, M., “Characterization

of steel mill electric-arc furnace dust", J. Hazard. Mater., 2004, B109, 59.
2. Machado, G. M. S., Brehm, F. A., Moraes, C. A. M., Santos, C. A., Vilela, A. C. F., and Cunha, J. B. M., "Chemical, Physical, Structural, and Morphological characterization of the electric arc furnace dust", J. Hazard. Mater., 2006, B136, 953.
3. Ruiz, O., Clemente, C., Alonso, M., and Alguacil, F. J., "Recycling of an electric arc furnace flue dust to obtain high grade ZnO", J. Hazard. Mater., 2007, 141, 33.
4. Best, T. E., and Pickles, C. A., "The treatment of electric arc furnace baghouse dusts in carbon monoxide", Metallurgical Processes for the Early Twenty-First Century Vol I: Basic Principles (Ed. H. Y. Sohn), TMS, 1994, 543.
5. Lopez, F. A., Medina, F., Medina, J., and Palacios, M. A., "Process for recovery of non-ferrous metals from steel mill dusts involving pelletising and carbothermic reduction", Ironmaking and Steelmaking, 1991, 18, (4), 292.
6. Guézennec, A. G., Huber, J. Ch., Patisson, F., Sessiecq, P., Birat, J. P., and Ablitzer, D., "Dust formation in electric arc furnace: birth of the particles", Powder Technol., 2005, 157, 2.
7. Bruckard, W. J., Davey, K. J., Rodopoulos, T., Woodcock, J. T., and Italiano, J., "Water leaching and magnetic separation for decreasing the chloride level and upgrading the zinc content of EAF steelmaking baghouse dusts", Intl. J. Min. Proc., 2005, 75, (1-2), 1.
8. Delalio, A., Bajger, Z., Balaz, P., and Castro, F., "Production of magnetite powder and recovery of non-ferrous metals from steel making residues", Proceedings of the XXI International Mineral Processing Congress, Vol. 13, 2000, C12a-15-C12a-19.
9. Kashiwaya, Y., Tsubone, A., Ishii, K., and Sasamoto, H., "Thermodynamic analysis on the dust generation from EAF for the recycling of dust, ISIJ International, 2004, 44, 1774.
10. Youcai, Z., and Stanforth, R., "Integrated hydrometallurgical process for production of zinc from electric arc furnace dust in alkaline media", J. Hazard. Mater., 2000, B80, 233.
11. Jarupistthorn, C., Pimtong, T., and Lothongkum, G., "Investigation of kinetics of zinc leaching from electric arc furnace dust by sodium hydroxide", Mater. Chem. and Phys., 2002, 77, 531.
12. Leclerc, N., Meux, E., and Lecuire, J. M., "Hydrometallurgical recovery of zinc and lead from electric arc furnace dust using mononitrilotriacetate anion and hexahydrated ferric chloride", J. Hazard. Mater., 2002, b91, 257.
13. Xia, D. K., and Pickles, C. A., "Microwave caustic leaching of electric arc furnace dust", Min. Eng., 2000, 13, (1), 79.
14. Dutra, A. J. B., Paiva, P. R. P., and Tavares, L. M., "Alkaline leaching of zinc from electric arc furnace steel dust", Min. Eng., 2006, 19, (5), 478.
15. P., Oustadakis, P. E. Tsakiridis, A. Katsiapi and S. Agatzini-Leonardou, Hydrometallurgical process for zinc recovery from electric arc furnace dust (EAFD). Part I: Characterization and leaching by diluted sulphuric acid, J. Hazardous Mater., 2010, 179, 1.
16. Tsakiridis, P. E., Oustadakis, P., Katsiapi, A., and Agatzini-Leonardou, S., "Hydrometallurgical process for zinc recovery from electric arc furnace dust (EAFD). Part II: Downstream processing and zinc recovery by electrowinning, J. Hazardous Mater., 2010, 179, 8.
17. Pickles, C. A., "Thermodynamic analysis of the separation of zinc and lead from electric arc furnace dust by selective reduction with metallic iron", Separation and Purification Technology, 2008, 59, 115.
18. Donald, J. R., and Pickles, C. A., "Reduction of electric arc furnace dust with solid iron powder", Canadian Metallurgical Quarterly, 1996, 35, 255.
19. Pickles, C. A., "Thermodynamic analysis of the selective chlorination of electric arc furnace dust", J. Hazard. Mater., 2009, 166, 1030.
20. Lee, G. S., and Song, Y. J., "Recycling EAF dust by heat treatment with PVC", Mater. Eng., 2007, 20, 739.
21. Itoh, S., Tsubone, A., Matsubae-Yokoyama, K., Nakajima, K., and Nagasaka, T., "New EAF dust treatment process with the aid of strong magnetic field", ISIJ International, 2008, 48, 1339.
22. Pickles, C. A., "Thermodynamic analysis of the selective carbothermic reduction of electric arc

furnace dust", J. Hazard. Mater., 2008, 150, 265.
23. Chen, H. K., "Kinetic study on the carbothermic reduction of zinc oxide", Scand. J. Metall, 2001, 30, (5), 292.
24. Kim, B. S., Yoo, J. M., Park, J. T., and Lee, J. Ch., "A Kinetic study of the carbothermic reduction of zinc oxide with various additives", Mater. Trans., 2006, 47, (9), 2421.
25. Chen, H. K., and Yang, Ch. Y., "Effect of additives on carbothermic reduction of zinc oxide", J. Mater. Sci. Letters, 1999, 18, 1399.
26. H.S. Ray, Kinetic of Metallurgical Reactions, Oxford & IBH Publishing Co. PVT. LTD., 1993.
27. Bafghi, M. Sh., Adeli, M., and Mohammadi Nikoo, H., "Kinetics of carbothermic reduction of Iranian celestite ore", Iranian Journal of Materials Science and Engineering, 2004, 1(3), 9.
28. Gokarn, A. N., Pardhan, S. D., Pathak, G., and Kulkarni, S. S., "Vanadium-catalyzed gasification of carbon and its application in the carbothermic reduction of barite", Fuel, 2000, 79, 821.
29. Bafghi, M. Sh., Yarahmadi, A., Ahmadi, A., and Mehrjoo, H., "Effect of the type of carbon material on the reduction kinetics of barium sulfate", Iranian Journal of Materials Science and Engineering, 2011, 8(3), 1.
30. Abdel Halim, K. S., "Isothermal reduction behavior of Fe_2O_3/MnO composite materials with solid carbon, Mater. Sci. and Eng. A, 2007, 452-453, 15.